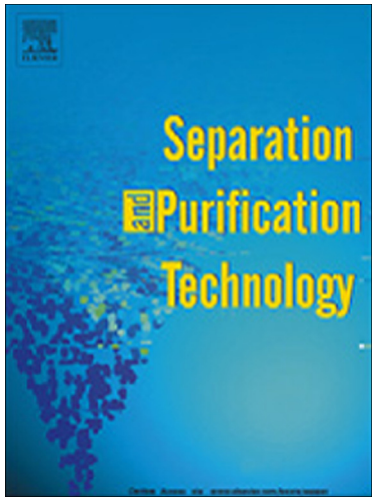

Improvement of Phosphorus Removal from Iron Ore Using Combined Microwave Pretreatment and Ultrasonic Treatment

Mamdouh Omran, Timo Fabritius, Ahmed M. Elmahdy, Nagui A. Abdel-Khalek, Stanislav Gornostayev

PII: S1383-5866(15)30320-8
DOI: http://dx.doi.org/10.1016/j.seppur.2015.10.071
Reference: SEPPUR 12675

To appear in: *Separation and Purification Technology*

Received Date: 13 August 2015
Revised Date: 26 October 2015
Accepted Date: 29 October 2015

Please cite this article as: M. Omran, T. Fabritius, A.M. Elmahdy, N.A. Abdel-Khalek, S. Gornostayev, Improvement of Phosphorus Removal from Iron Ore Using Combined Microwave Pretreatment and Ultrasonic Treatment, *Separation and Purification Technology* (2015), doi: http://dx.doi.org/10.1016/j.seppur.2015.10.071

Improvement of Phosphorus Removal from Iron Ore Using Combined Microwave Pretreatment and Ultrasonic Treatment

Mamdouh Omran[a,b*], Timo Fabritius[a], Ahmed M. Elmahdy[b], Nagui A. Abdel-Khalek[b], Stanislav Gornostayev[a]

[a] Process Metallurgy Research Group, Faculty of Technology, University of Oulu, Finland.

[b] Mineral Processing and Agglomeration Lab, Central Metallurgical Research and Development Institute, Cairo, Egypt.

Abstract

Most of the past studies examined the effects of ultrasonic treatment on the removal of phosphorus, silica and alumina minerals from iron ores. In the present work, the effect of combined microwave pretreatment and ultrasonic treatment on the efficiency of disintegration and removal of phosphorus and other gangue minerals associated with iron ores has been studied. Three different iron ore samples have varying total iron concentration (TFe) and P_2O_5 content and mineralogical textures were studied.

Microwave pretreatment generated intergranular fractures between the gangues (fluoroapatite and chamosite) and oolitic hematite. These intergranular fractures improved liberation of iron ore, and accelerated ultrasonic disintegration and removal of phosphorus and gangue minerals from oolitic hematite. The results indicated that microwave pretreatment increases the efficiency of ultrasonic disintegration and removal of particles by about 20% compared to untreated sample. The results of ultrasonic treatment are quite promising. Significant increase in iron grade and reduction in phosphorus and alumina content of enriched product can be obtained. Depending on the sample texture and phosphorus distribution, about 59 % phosphorus removal can be obtained.

Key words: Microwave pretreatment; Ultrasonic treatment; high phosphorus iron ore.

Corresponding author:

Mamdouh Omran

Address: Process Metallurgy Research Group, Faculty of Technology, University of Oulu, Finland.

P.O. Box: 4300.

E-mail: mamdouh.omran@oulu.fi

1. Introduction

There is a rapidly increasing demand for iron resources with the rapid development of iron and steel industry, therefore iron and steel industry facing the risk of raw material shortage. Deposits of high phosphorus oolitic iron ores are widely spread worldwide [1-7]. The main obstacle associated with exploiting these deposits is the fine dissemination of silica, aluminum and in particular phosphorus minerals, which affects the economy of iron making process and the quality of the produced steel. Song et al. [8] observed that fine grinding (commonly 1–5 μm) is required to liberate iron minerals from associated gangue minerals. Such fine particles are very difficult to beneficiate via conventional mineral processing operations. For upgrading high phosphorus oolitic iron ores, many hydrometallurgical and pyrometallurgical processes were proposed [9-15]. Although some of these methods achieved the purpose of phosphorus removal, they suffer from some disadvantages. For instance, low efficiency of dephosphorization, environmental pollution, relatively high cost, and low iron recovery represent drawbacks that make these techniques impractical. The development of a successful and economic process to remove phosphorus from the high phosphorus iron ores would significantly extend the reserves of high grade low phosphorus iron ores, and develop iron and steel industries [16].

A growing interest in microwave heating in mineral treatment has emerged in recent years, and a number of potential applications regarding microwave processing have been investigated [17-21]. Microwave treatment improves the liberation of high phosphorus oolitic iron ores by generating intergranular fractures in oolitic iron ores [8]. The difference in the absorption of microwave energy, thermal expansion and the dielectric properties of iron and gangue minerals leads to the generation of intergranular fractures between iron and gangue minerals [17, 22 - 25]. High phosphorus oolitic iron ores are usually composed of hematite, dolomite, clinochlore, quartz and apatite (fluoroapatite or hydroxyl fluoroapatite), these minerals differ in how they absorb microwave energy [15]. These minerals have different reactions regarding thermal expansion, and thus thermal stresses are generated on the boundaries between them. When these thermal stresses reach a critical level, cracks and fissures are formed at the boundaries [26]. Omran et al. [27-28] studied the influence of microwave pre-treatment on the liberation of high phosphorus oolitic iron ore. They concluded that intergranular fractures formed between the gangues (fluoroapatite and chamosite) and oolitic hematite after microwave treatment, leading to improved liberation of iron ore [27-28]. Omran et al. [27-30] concluded that compared to conventional thermal treatment, microwave treatment consumes considerably less energy, improves liberation and reduces processing time. Many researchers investigated the influence of microwave pre-treatment on magnetic separation and surface characteristics of ores [31–33]. They concluded that microwave treatment of ores is potentially high efficient pre-treatment technique with low energy consumption [31-33].

In the present study, ultrasonic treatment was applied to the microwave treated samples with the aim of investigating the effect of combined microwave pre-treatment and ultrasonic treatment on the separation of phosphorus and other gangue minerals from iron ore.

When ultrasonic waves are propagating through liquid, vibrations in the medium create a series of rarefactions and compressions that initiates nucleation of micro-bubbles ″cavitation″. These

cavitations take place primarily on the phase boundary since solid/liquid interactions are weaker than liquid cohesion forces [34-39]. When high temperature and pressure are attained inside the cavitation bubbles, their diameter exceeds a critical value, they collapse asymmetrically in the vicinity of solids present within the liquid [34-41]. Asymmetric collapse leads to the formation of high speed micro-jets that have the potential to remove the gangue constituents adhered on the surface of iron mineral particles [40, 41].

Donskoi et al. [41-48] extensively studied the effect of ultrasonic treatment on upgrading of iron ore. They concluded that it is possible to increase iron grade and recovery if hematitic/goethitic iron ore treated with ultrasound [41]. They also found that the application of ultrasound with stirring have a significant effect on the product grade [43]. Ozkan [49] reported that recovery values of magnesite slimes increased with ultrasonic treatment. Franko and Klima [38] have concluded that ultrasonic treatment helped to separate ultra-fines attached to larger particles in iron ore beneficiation processes. Pandey et al. [40] also reported that ultrasonic treatment followed by de-sliming significantly reduced alumina, silica and phosphorus for two Indian iron ores.

The findings of the previous studies [8, 27-33] indicated that microwave heating can improve the liberation, grindability, and magnetic separation of valuable minerals from ores and has a potential to provide a new method to treat ores successfully. The aim of this investigation is to study the effect of microwave pretreatment on the effectiveness of ultrasonic disintegration and separation of phosphorus and other gangues minerals from iron ores. The hypothesis of using combined microwave pretreatment and ultrasonic treatment is that intergranular fractures formed between the gangues and oolitic hematite grains after microwave treatment, when ultrasonic treatment applied to the microwave treated sample, these intergranular fractures facilitate ultrasonic waves to remove the gangue constituents adhered on the surface of iron mineral particles.

2. Experimental and materials

2.1. Iron ore samples

The iron ore samples used in this study were collected from Aswan region, Egypt. Eastern Aswan area represents the main occurrence of the Cretaceous ironstone bands of South Egypt [6, 7]. Three different samples were obtained from different locations from Aswan region.Tables (1 and 2) show the chemical and mineralogical analysis of the iron ore samples investigated in this study. The main mineral phase found in all samples is hematite as the main iron bearing mineral. The main associated gangue minerals are fluorapatite, quartz and chamosite.

2.2. Microwave treatment

Samples were treated using a 2.45 GHz microwave oven with 900 Wmaximum output power. Three representative samples with grain size in the range (-1000μm +500μm), (-500μm +250 μm) and (-250 μm +125 μm) were used in each test. Iron ore samples were treated under normal atmosphere condition and directly used without any pretreatment. Samples were placed in the microwave oven in crucibles made of pure alumina. The temperature of each sample was measured by quickly inserting a thermocouple into the sample after the power was turned off, and the temperature was monitored by a digital display temperature controller. The measured temperatures are the bulk temperature of the samples (Fig. 1). The samples were then allowed to cool in the microwave oven to room temperature.

2.3. Ultrasonic treatment

An ultrasonic cleaning vessel (Elmasonic P30H) with ultrasonic frequency 37 kHz and ultrasonic power 350 W was used. The internal dimensions of ultrasonic tank are (240 × 137 × 100 mm). The experimental setup is shown in Fig. (2). The pulp sample was placed in the experimental vessel

together with an impeller (for stirring) in the ultrasonic bath. A schematic diagram of the process flow sheet is shown in Fig. (3).

The impeller rotation speed was varied from 350 rpm to 700 rpm and it was observed that with increasing rotation speed the power transferred from the ultrasonic probe decreased [41]. The impeller rotation speed was then fixed at 350 rpm in all experiments. Different pulp densities (15%, 30% and 45%) and different ultrasonic treatment times (5, 10, 20, 30 minutes) were applied to investigate the effect of sonication time and pulp density on the performance of ultrasonic disintegration and gangues minerals removal. Samples with different grain sizes were tested to determine the effect of particles size on the efficiency of ultrasonic treatment.

After ultrasonic treatment, the pulp was de-slimed through – 63 μm, dried, weighed and chemically analyzed. From the chemical analyses of preliminary experiments, it was found that the -37μm fraction is rich in P and Al whereas -63μm +37μm fraction is rich in Si. Fractions above 63μm have P and Al ratios similar to the feed sample. Based on these results, -63μm size fraction was used to represent the percentages of disintegration materials.

2.4. Analytical techniques

The mineralogical composition of the feed and the products samples of ultrasonic experiments were performed on powdered samples using a Siemens D5000 XRD powder diffractometer. The device contains a Cu Kα radiation with a graphite monochromator. The XRD analyses were made using 40 KV and 40 mA. Chemical analyses for feed and product samples were performed on whole rock powders by X-ray fluorescence (Bruker AXS S4 Pioneer). The micro-morphological characteristics of the ore before and after treatment with microwave and ultrasonic were investigated using a Zeiss ULTRA plus field emission scanning electron microscope (FESEM), which was attached to an energy-dispersive X-ray spectroscopy (EDS) unit for chemical analysis.

3. Results and discussion.

3.1. Material characterization

The chemical and mineralogical analysis of selected grain size fractions of the three representative samples were listed in Tables 1 and 2, respectively. These samples have different mineralogical textures, Fe_2O_3 and P_2O_5 percentages. Based on the chemical compositions and samples texture, the ore samples are classified into three types:

1- High phosphorus sample (G1), TFe (48.33%) and P_2O_5 (5.64 %).

SEM images show that Fe-bearing minerals occur mainly as fine-grained cement-like materials mixed with phosphorus bearing mineral and detrital quartz (Figs. 4A - 4D). Also hematite occurs as small ooid grains (Fig. 4A). SEM analyses indicated that the sample texture occurs as sandy and silty ironstones (ferruginous sandstone and siltstone). EDX analyses indicated that phosphorus occurs as very fine grains disseminated in fine iron mineral (Figs. 4B and 4D).

2- Low phosphorus sample (G2), TFe (46.08%) and P_2O_5 (2.25 %).

SEM images show that the sample composed mainly of ooiltic hematite and detrital quartz (Figs. 5A and 5B). Chamosite and Fluoroapatite occur mainly as cement-like materials mixed with quartz and iron filling the spaces between ooid grains (Figs. 5A - 5D). SEM and EDX analyses indicated that the sample texture occurs as oolitic ironstones, and most gangue minerals (fluoroapatite and chamosite) concentrated in the spaces between ooids.

3- Intermediate phosphorus sample (G3), TFe (58.27%) and P_2O_5 (3.24 %).

SEM images show that Fe-bearing minerals occur as oolitic hematite with less abundant phosphates and ferruginous clayey materials “chamosite” (Fig. 6A). Fluoroapatite (phosphorus bearing mineral) occurs mainly as a fine-grained material fills the spaces between ooid grains (Figs. 6B - 6D). Chamosite occurs as a rim surrounding (coating) the ooid grains (Figs. 6B - 6D). SEM and EDX analyses showed that the sample has a true

oolitic ironstone texture and phosphorus concentrated mainly in the interstitial spaces between ooids (Figs. 6B - 6D).

3.2. Microwave pretreatment of high phosphorous oolitic iron ore.

The influence of different microwave heating parameters on the generation of intergranular fractures between oolitic hematite and gangues minerals, and its effect on liberation were investigated by Omran et al. [27, 28]. As explained by the previous theoretical studies concerning microwave treatment of ores, the main reason of the damage after microwave treatment is the thermally-induced tensile stress, which occurred during the thermal expansion of the absorbent phases, exceeding the tensile strength of the material [18, 20, 23, 25, 50, 51, 52]. Hematite is an active material to microwave heating, while gangues (fluoroapatite, chamosite and quartz) are inactive materials. When hematite exposed to microwave radiation, it expanded more than gangues. This difference in expanding results in the formation of intergranular fractures [8]. Table (3) indicates the heating properties of hematite and gangue minerals with microwave radiation [53].

For sample (G3), after microwave treatment at the optimum heating conditions (60 s exposure time and 900 W microwave power) [27, 28], intergranular fractures formed between the gangues (fluoroapatite and chamosite) and oolitic hematite and almost no damages in the oolite grains Fig. (7). At this stage, oolites are mostly liberated from the matrix which means that most of phosphorus can be removed Fig. (7D). In case of sample (G2), fractures are formed on the boundaries between the gangues and oolitic hematite after microwave treatment (Fig. 8A and 8B). Also fractures appeared in the matrix between ooids (Fig. 8C and 8D). These intergranualr fractures facilitate phosphorus separation. On the other hand, sample G1, micro-cracks were observed in the fine grained materials and between the small dispersed oolites and matrix (Fig. 9).

Omran et al. [27, 28] concluded that the behavior of samples during microwave heating was different in terms of the generation of intergranular fractures. Sample mineralogical texture affected the degree of liberation of iron minerals from associated phosphorus. Samples (G2 and G3) affected

significantly by microwave heating more than sample (G1). Samples (G2 and G3) have coarse grains (oolitic ironstones) texture, while sample (G1) has fine-grained texture. It was observed that the effect of microwave heating increased by increasing grain size [21-25].

3.3. Effect of microwave pretreatment on ultrasonic treatment efficiency

The difference of the effect of ultrasound on iron ore pretreated with microwave and on iron ore without microwave pretreatment is quite obvious (Table 4). The amounts of disintegration materials (- 63 μm) generated from samples without microwave pretreatment are significantly lower than that generated from microwave pretreated samples (Table 4). This may be due to intergranular fractures generated between the gangues (fluoroapatite, quartz and chamosite) and oolitic hematite after microwave treatment [27, 28]. These intergranular fractures improved liberation, facilitate ultrasonic disintegration and removal of phosphorus and gangue minerals from the surface of oolitic hematite. These observations indicated that microwave pretreatment should be considered as a factor significantly affecting the results of ultrasonic treatment.

What is interesting to emphasize is that the effect of ultrasonic on samples (G2 and G3) is stronger than on sample (G1) under the same experimental conditions. The reason for the difference in ultrasonic effects between samples is related to samples texture. The behaviour of samples during microwave pretreatment were different in terms of the generation of intergranular fractures, as indicated previously. The difference between the amounts of disintegration materials generated from iron ore samples without and with microwave pretreatment is significant on samples (G2 and G3) compared to sample (G1). As a result, samples (G2 and G3) are more affected by microwave pretreatment than sample (G1). For example, the amount of disintegration materials generated from untreated samples are (12.22 -12.44%) for samples (G2 and G3), respectively (Table 4). While the amount of disintegration materials generated from microwave treated samples are (14.44 -15.48%) from samples (G2 and G3), respectively (Table 4). It's clear from these results, microwave

pretreatment increases the rate of ultrasonic disintegration and removal of particles by about (20 % compared to untreated sample). While the amount of disintegration materials increased only about (10 % compared to untreated sample) for sample (G1) (Table 4).

The results indicates that the effectiveness of disintegration and fine removal was higher for microwave treated samples in comparison with samples treated with ultrasonic only.

3.4. Ultrasonic treatment of high phosphorus iron ore

Several parameters (e.g. sample grain size, sonication time and pulp density) were studied to achieve optimum conditions. From preliminary experiments, ultrasonic treatment without stirring has very low efficiency as the ore creates a dense cake on the bottom of the cell with low permeability for the ultrasonic waves resulting in low level of cavitation. It was found that for ultrasonic to be efficient the ore should be suspended in water or stirred [41].

3.4.1. Effect of sonication time.

The influence of ultrasonic treatment time on the disintegration and removal of fine particles was studied (Figs.10-12). According to Figs. (10-12), increasing ultrasonic exposure time resulted in increasing the amounts of disintegrated materials (- 63μm).

The effect of ultrasound on the three samples was different. Figures (10-12) show that the percentage of disintegrated materials generated from sample (G1) is significantly lower (8.82%) than for samples G2 and G3 (11.54% and 12.54%, respectively) under the same conditions (5 min of ultrasonic treatment, +125 -250 μm particles size). The effectiveness of ultrasonic disintegration significantly decreases with increasing ultrasonic time. For example, the amount of fine materials

generated for sample (G2, +125 -250 μm) after ultrasonic treatment for duration of 10 and 30 minutes was 15.48% and 24.66 %, respectively (Fig. 10).

Figs. (13-15) show the effect of different ultrasonic treatment times on total iron grade and decreasing the impurities such as phosphorous, alumina and silica. From all these graphs it is obvious that iron grade increases while gangues grade decreases at the optimum ultrasonic treatment time. This is due to disintegration and removal of fine materials (which are lower in iron grade and higher in phosphorus and gangues contents) from the coarser fractions. Researchers [40, 41] investigated that longer ultrasonic treatment time resulted in decreasing iron grade, due to disintegration of soft hematite.

Tables (5 and 6) presented the chemical and mineralogical analyses for the three studied samples at optimum ultrasonic treatment times.

For sample (G2), the optimal time of treatment was 5 min, after which the level of phosphorus and alumina in the de-slimed product increased again (Fig. 13). This behavior was observed also by Pandy et al. [40]. The chemical composition of sample G2 products after ultrasonic treatment shows that the percentage of iron has increased from 45.35% to 48.32%. On the other hand, phosphorus, alumina and silica decreased from 1.45%, 2.41% and 33% (feed sample with microwave pretreatment) to 0.71%, 1.18% and 29% (de-slimed product), respectively. Reduction in phosphorus and alumina is more significant than silica because their bearing minerals are softer than silica and are easier to be broken by ultrasonic. The total reduction of phosphorus, and alumina compared to the initial ore are 68% and 51%, respectively.

The mineralogical analysis of the original and treated ore sample (G2), are shown in Table (6). It can be seen that the percent of hematite has significantly increased after ultrasonic treatment (from 59% to 71%). The amount of fluoroapatite and chamosite (iron clay) have significantly decreased (from 3% to 1% and from 6% to 3%, respectively).

Figure (14) shows that sample (G3) has the most significant increase in iron grade and reduction in phosphorus and alumina content after 10 minutes of ultrasonic treatment. Longer ultrasonic treatment times caused the iron grade to be significantly reduced. The chemical composition shows that the iron grade has increased from 58.50 % to 60.58 %. Phosphorus and Alumina decreased from 2.79 % to 1.88% and from 4.12 % to 2.86 %, respectively. While silica decreased from 8.66% to 7.22%. The removal percent of phosphorus and alumina is 32 % and 30 %, respectively. The total reduction of phosphorus, and alumina compared to the initial ore are 42% and 36%, respectively.

The mineralogical analysis for the products of sample (G3) is shown in Table (6). It can be seen that hematite increased after ultrasonic treatment (from 74% to 82%) while fluoroapatite and chamosite (iron clay) were decreased (from 8.69% to 5.91% and from 10.30% to 7.21%, respectively).

The chemical analysis of sample (G1) (Fig. 15 and Table 5) indicates that ultrasonic treatment has insignificant effect on iron grade and gangue minerals removal after ultrasonic treatment. It can be noticed that the iron grade has increased from 47.97% to 48.66% while phosphorus and Alumina decreased from 3.17% and 3.40% to 2.58% and 2.42%, respectively.

3.4.2. Effect of Particle size

The effect of particles size on the amount of disintegrated materials is shown in Figs. (10-12). The effect of ultrasonic treatment on larger particles is significantly lower than smaller particles. For example, under the same experimental conditions (5 min of ultrasonic treatment, 15% pulp density), the amount of disintegrated materials generated using sample (G3) with particle size (+125 -250 μm) was 11.54 % compared to 9.34 % using sample with particle size (+250 -500 μm), (Fig. 11). The reason for decreasing the amount of disintegrated materials with larger particle size was explained by their lower surface area so the effect of ultrasound is expected to be also lower [41, 43].

It is noted that the effectiveness of disintegration and fines removal was much lower with further increase in particle size up to (+500 – 1000 μm). The percentage of disintegration materials generated using sample (G3) decreased to 2.66 %. The large particles (+500 – 1000 μm) partially settled on the bottom of the cell, resulting in low permeability for the ultrasonic waves, this causes low level of cavitation and significant reduction in the ultrasonic effect [41].

3.4.3. Effect of Pulp density

The effect of sonicating at various solid/liquid ratios (pulps density) was investigated (Table 7). It can be seen that the pulp density has minor effect on material disintegration. Donskoi et al. [41, 46] concluded that the effect of ultrasound on pulps of low density is slightly larger than on high density pulps.

At fixed ultrasonic treatment time (10 min), pulp density was tested at 15% and 45% pulp densities. The amount of material generated in sample G3 having particle size +125 μm -250 μm with 15% pulp density was 14.62% compared to 10.44% using 45% pulp density under the same conditions (Table 7). This result indicated that, although the pulp density of sample increased three times, the difference in the amount of disintegrated material decreased only by about 4%. It can be concluded that the pulp density has minor effect on the performance of ultrasonic disintegration and removal of gangue minerals [41]. The effect of different pulp densities on the three different samples at different size fractions is shown in Table 7.

3.5. The effect of ore texture on ultrasonic treatment performance

Egyptian high phosphorus iron ores have different textural and liberation characteristics. Phosphorus and other gangue minerals (silica and alumina) may be present as either liberated, locked or coating of the hematite grains. In order to design an ultrasound treatment for complex ores, such as oolitic iron ore, a perfect knowledge of the ore texture and mineralogy is needed [42].

Samples (G2 and G3) have oolitic ironstones texture, and most gangue minerals (fluoroapatite, quartz and chamosite) are concentrated in the interstitial spaces as coating ooid grains (Figs. 5 and 6). When samples exposed to ultrasonic treatment, phosphorus and gangue minerals removed from the surface of ooid grains. This behavior might be due to that the interfaces between oolitic hematite and gangue minerals' particles are potential sites for transient cavitation. Microwave energy can selectively break the bonds between the gangues and oolitic hematite particles and liberate phosphorus and other gangues from the hematite surface [40].

While in case of sample G1, iron texture occurs mainly as fine-grained cement-like materials mixed with phosphorus (locked) Fig. (4). This sample texture reduce the effect of both microwave pretreatment and ultrasonic treatment on phosphorus removal.

SEM images confirmed that preferential disintegration of soft gangue minerals (fluoroapatite and chamosite) from the oolites surface occurs during ultrasonic treatment (Figs. 16 and 17). Figures (16-17 A and B) show SEM images of samples G2 and G3, respectively, without ultrasonic treatment. It is clear that most gangue minerals (fluoroapatite and chamosite) coating hematite ooid grains. After ultrasonic treatment, as shown in Figs. (16-17 C and D), the effect of ultrasonic treatment is clearly indicated by disintegration of gangue minerals (fluoroapatite and chamosite) from the surface of hematite. Figs. (16-17 C and D) indicate that most phosphorus and alumina (fluoroapatite and chamosite) particles have been detached after ultrasonic treatment.

It can be concluded that, the efficiency of ultrasonic removal of phosphorus depends on sample grain size texture and the degree of phosphorus liberation. For Samples (G2 and G3) have large grain oolitic texture and phosphorus coating oolitic grains (liberated). While sample G1, iron texture occurs as fine-grained cement-like materials mixed with phosphorus (locked). It can be seen that total iron grade of the products for samples (G2 and G3) is higher than that for untreated ore by 2 to 3% (Table 5). The percentage of phosphorus removal with ultrasonic treatment after microwave pretreatment for samples G2 and G3 is 59 % and 33%, respectively. While for sample

(G1) there is no significant difference in iron grade after ultrasonic treatment and only 18% of phosphorus removed after ultrasonic treatment (Table 5).

Conclusions

The possibility of phosphorus removal from high phosphorus iron ore using combined microwave pretreatment and ultrasonic treatment was studied. The results indicated that microwave pretreatment significantly increases the efficiency of ultrasonic disintegration and the removal of gangues. The improvement in Fe grade and the decrease in impurities after ultrasonic treatment is attributed to the disintegration and removal of fine gangue components.

The experiments indicated that excessive ultrasound treatment has a negative impact on the product quality. Disintegration of fine gangue mineral particles decreases with increasing sample particle size and pulp density under similar sonication conditions.

It was found that mineralogical texture and the degree of phosphorus liberation affect the efficiency of phosphorus removal.

Acknowledgments

The authors acknowledge (Cultural Affair and Mission Sector, Egypt) and CIMO (Center for International Mobility, Finland) for their financial grant for performing the present research work. The authors are indebted to Prof. Ali Abdelmotelib from geology Department, Cairo University for his assistance during sample collection from Aswan region, Egypt. The authors thank Mr. Riku Mattila and Mr. Tommi Kokkonen for their technical support throughout this work.

References

[1] A.A. Manieh, Oolite liberation of oolitic iron ore,Wadi Fatima, Saudi Arabia, Int. J. Miner. Process. 13 (1984) 187 - 192.

[2] Y. Champetier, E. Hamdadou, M. Hamdadou, Examples of biogenic support of mineralization in two oolitic iron ores—lorraine (France) and garadjebilet (Algeria), Sediment. Geol. 51 (1987) 249 -255.

[3] O. Ozdemir, E.R. Deutsch, Magnetic properties of oolitic iron ore on Bell Island, New found land, Earth Planet. Sci. Lett. 69 (1984) 427- 441.

[4] M.M. Abro, A.G. Pathan, A.H. Mallah, Liberation of oolitic hematite grains from iron ore, DilbandMines Pakistan, Mehran University Research, J. Eng. Technol. 30 (2011) 329 - 338.

[5] K. Li, W. Ni, M. Zhu, M. Zheng, Y. Li, Iron extraction from oolitic iron ore by a deep reduction process, J. Iron Steel Res. Int. 18 (2011) 9 - 13.

[6] M.A. EL Sharkawi, M.M. EL Aref, A.A. Mesaed, Stratigraphic setting and paleoenvironment of the Conician Santonian ironstones of Aswan, Geological Society of Egypt, South Egypt, Special Publication No. 2, (1996) 243 - 278.

[7] M.M. El Aref,M.A. EI Sharkawi, A.A. Mesaed, Depositional and diagenetic microfabric evolution of the cretaceous oolitic ironstone of Aswan, Geological Society of Egypt, Egypt, Special Publication No. 2, (1996) 279 - 312.

[8] S. Song, E.F. Campos-Toro, A.L. Valdivieso, Formation ofmicrofractures on an oolitic iron ore under microwave treatment and its effect on selective fragmentation, Powder Technol. 243 (2013) 155 - 160.

[9] J. Ji, Study on Dephosphorization Technology for High-Phosphorus Iron Ore, Mining & Metallurgy. 12(2003) 33-37.

[10] W.T. Xia,Z.D. Ren, Y.F. Gao, Removal of Phosphorus from High Phosphorus Iron Ores by Selective HCl Leaching Method, Int. J. Iron Steel Res. 18(2011) 1-4.

[11] C.Y. Cheng,V.N.Misra, J.Clough, R.Muni, Dephosphorisation of Western Australian Iron Ore by Hydrometallurgical Process, Miner, Eng. 12(1999) 1083-1092.

[12] J.C. Wang, S.B. Shen, J.H.Kang, H.X.Li, Z.C. Guo, Effect of Ore Solid Concentration on the Bioleaching of Phosphorus from High-Phosphorus Iron Ores Using Indigenous Sulfur-Oxidizing Bacteria from Municipal Wastewater, Process Biochem. 45 (2010) 1624-1631.

[13] P.Delvasto, A.Valverde, A.Ballester, J.A. Munoz, F. Gonzalez, M.L.Blazquez, Diversity and Activity of Phosphate Bioleaching Bacteria from a High-Phosphorus Iron Ore, Hydrometallurgy 92(2008) 124-129.

[14] Y.F. Yu, C.Y. Qi, Magnetizing Roasting Mechanism and Effective Ore Dressing Process for Oolitic Hematite Ore. Journal of Wuhan University of Technology, Materials Science Ed., 26(2011) 176-181.

[15] H.Q.Tang, Z.C. Guo, Z.L. Zhao, Phosphorus Removal of High Phosphorus Iron Ore by Gas-Based Reduction and Melt Separation, Int. J. Iron Steel Res. 17(2010) 1-6.

[16] M.J.Fisher-White, R.R.Lovel, G.J. Sparrow, Phosphorus Removal from Goethitic Iron Ore with a Low Temperature Heat Treatment and a Caustic Leach, ISIJ International 52 (2012) 797 - 803.

[17] S.W. Kingman, N.A. Rowson, Microwave treatment of minerals—a review, Miner. Eng. 11 (1998) 1081 - 1087.

[18] K. Barani, S.M.J. Koleini, B. Rezaei, Magnetic properties of an iron ore sample after microwave heating, Sep. Purif. Technol. 76 (3) (2011) 331 - 336.

[19] G. Roussy, J.A. Pearce, Foundations and industrial applications ofmicrowave and radiofrequency fields, Physical and Chemical Processes, Wiley, 1995. (Chapters 10, 11, 12).

[20] K.E. Haque, Microwave energy for mineral treatment processes—a brief review, Int. J. Miner. Process. 57 (1) (1999) 1 - 24.

[21] D.A. Jones, T.P. Lelyveld, S.D. Mavrofidis, S.W. Kingman, N.J. Miles, Microwave heating applications in environmental engineering—a review, Resour. Conserv. Recycl. 34 (2002) 75 - 90.

[22] K.E. Fitzgibbon, T.J. Veasey, Thermally assisted liberation—a review,Miner. Eng. 3 (1/2) (1990) 181 - 185.

[23] D.A. Jones, S.W. Kingman, D.N. Whittles, I.S. Lowndes, Understanding microwave assisted breakage, Miner. Eng. 18 (2005) 659 - 669.

[24] D.N. Whittles, S.W. Kingman, D.J. Reddish, Application of numerical modelling for prediction of the influence of power density on microwave-assisted breakage, Int. J. Miner. Process. 68 (2003) 71 - 91.

[25] D.A. Jones, S.W. Kingman, D.N. Whittles, I.S. Lowndes, The influence of microwave energy delivery method on strength reduction in ore samples, Chem. Eng. Process. Process Intensif. 46 (4) (2007) 291 - 299.

[26] H.Q. Tang, J.W.Wang, Z.Ch. Guo, O. Tie, Intensifying gaseous reduction of high phosphorus iron ore fines by microwave pretreatment, J. Iron Steel Res. Int. 20 (5) (2013) 17 - 23.

[27] M.Omran, T. Fabritius, N. Abdel-Khalek, M.El-Aref, A.E.-H.Elmanawi, M. Nasr, A.Elmahdy, Microwave Assisted Liberation of High Phosphorus Oolitic Iron Ore, J. Miner. Mater.Charact. Eng. 2 (2014) 414-427.

[28] M. Omran, T. Fabritius, R. Mattila, Thermally assisted liberation of high phosphorus oolitic iron ore: Comparison between microwave and conventional furnace, Powder Technol. 269 (2015) 7 - 14.

[29] M. Omran, T. Fabritius, N. Abdel-Khalek, A. Elmahdy, Effect of microwave pretreatment on the magnetic properties of iron ore and its implication on magnetic separation, Sep.Purif. Technol. 136 (2014) 223 - 232.

[30] M. Omran, T. Fabritius, N. Abdel-Khalek, A. Elmahdy, XPS and FTIR Spectroscopic Study on Microwave Treated High Phosphorus Iron Ore, App. Surf. Sci. 345 (2015) 127 - 140.

[31] W. Zhao, J. Chen, X. Chang, S. Guo, C. Srinivasakannan, G. Chen, J. Peng, Effect of microwave irradiation on selective heating behavior and magnetic separation characteristics of Panzhihua ilmenite, App. Surf. Sci. 300(2014) 171 - 177.

[32] G. Chen, J. Chen, S. Guo, J. Li, C. Srinivasakannan, J. Peng, Dissociation behavior and structural of ilmenite ore by microwave irradiation, App. Surf. Sci. 258(10) (2012) 4826-4829.

[33] G. Chen, J. Chen, J. Li, S. Guo, C. Srinivasakannan, J. Peng, Optimization of combined microwave pretreatment-magnetic separation parameters of ilmenite using response surface methodology, Powder Technol. 232 (2012) 58-63.

[34] E.C. Cilek, S.Ozgen, Effect of ultrasound on separation selectivity and efficiency of flotation, Miner. Eng. 22 (2009) 1209 – 1217.

[35] M.S. Celik, Effect of ultrasonic treatment on the floatability of coal and galena, Sep. Sci. Technol. 24 (14) (1989) 1159- 1166.

[36] H.Kursun,A Study on the Utilization of Ultrasonic Pretreatment in Zinc Flotation, Sep. Sci. Technol. 49:18(2014) 2975-2980.

[37] T.J.Mason, J.P. Lorimer, Sonochemistry, Theory, Applications and Uses of Ultrasound in Chemistry. Ellis Horwood Publishers, 1991, London.

[38] J. Franko, M.S. Klima, Application of ultrasonics to enhance wet-drum magnetic separator performance, Miner. Metall. Process. 19 (1) (2002) 17 - 20.

[39] A.D.Farmer, A.F. Collings, G.J. Jameson, Effect of ultrasound on surface cleaning of silica Particles, Int. J. Miner. Process. 60 (2000) 101-113.

[40] J.C. Pandey, M. Sinha, M. Raj, Reducing alumina, silica and phosphorous in iron ore by high intensity power ultrasound,Ironmak. Steelmak. 37 (8) (2010) 583–589.

[41] E. Donskoi, A.F. Collings, A. Poliakov, W.J. Bruckard, Utilisation of ultrasonic treatment for upgrading of hematitic/goethitic iron ore fines, Int. J.. Miner. Process. 114 -117 (2012) 80 - 92

[42] E.Donskoi, S.P.Suthers, J.J. Campbell, T.Raynlyn, J.M.F. Clout, Prediction of hydrocyclone performance in iron ore beneficiation using texture classification. Proceedings XXIII International Mineral Processing Congress, Istanbul,(2006a) 1897–1902.

[43] E.Donskoi, J.J. Campbell, J.M. Young, T. Raynlyn, Experimental study of attrition effects in a hematite–goethite iron ore during hydrocycloning. Proceedings XXIII International Mineral Processing Congress, Istanbul, (2006b) 50 - 55.

[44] E.Donskoi, S.P.Suthers, S.B.Fradd, J.M. Young, J.J. Campbell, T.D.Raynlyn, J.M.F. Clout, Utilization of optical image analysis and automatic texture classification for iron ore particle characterisation. Miner. Eng. 20 (2007a) 46 - 471.

[45] E.Donskoi, J.J. Campbell, J.M. Young, T.Raynlyn, A.Poliakov, Examination of ultrasonic treatment of iron ore fines using automatic iron ore texture classification. Proceedings, Iron Ore 2007, Fremantle, WA, Australia (2007b) 251 - 257.

[46] E.Donskoi, S.P.Suthers, J.J. Campbell, T.Raynlyn, Modelling and optimization of hydrocyclone for iron ore fines beneficiation — using optical image analysis and iron ore texture classification, Int. J. Miner. Process. 87 (2008a) 106 - 119.

[47] E.Donskoi, R.J. Holmes, J.R. Manuel, J.J. Campbell, A.Poliakov, S.P.Suthers, T.Raynlyn, Utilization of iron ore texture information for prediction of downstream process performance, Proceedings, 9th International Congress for Applied Mineralogy, Brisbane, Australia (2008b) 687 - 693.

[48] E. Donskoi, A. Poliakov, J.R.Manuel, T.D.Raynlyn, Advances in optical image analysis and textural classification of iron ore fines, Proceedings, XXV International Mineral Processing Congress - IMPC2010, Brisbane, Australia (2010) 2823 - 2836.

[49]S. G. Ozkan, Beneficiation of magnesite slimes with ultrasonic treatment, Minerals Eng.15(2002) 99 - 101.

[50] A.Y.Ali,S.M.Bradshaw, Quantifying Damage around Grain Boundaries in Microwave Treated Ores, Chem. Eng. Processing: Process Intensification 48(2009) 1566-1573.

[51] A.Y.Ali, S.M. Bradshaw,Bonded Particle Modelling of Microwave Induced Damage in Ore Particles, Miner. Eng. 23 (2010) 780-790.

[52] J.B.Salsman, R.L.Williamson, W.K.Tolley, D.A.Rice, Short Pulse Microwave Treatment of Disseminated Sulphide Ores, Miner. Eng. 9(1996) 43-54.

[53] T.T.Chen, J.E.Dutrizac, K.E.Haque, W.Wyslouzil,S,Kashyap, The Relative Transparency of Minerals to Microwave Radiation, Canadian Metallurgical Quarterly 23(1984) 349-351.

List of figures

Fig. (12) Effect of sonication time on the percentages of disintegration materials for sample (G1). (15% pulp density).

Fig. (13) Effect of different ultrasonic treatment times on Fe grade and impurities phosphorous, alumina and silica for sample (G2).

Fig. (14) Effect of different ultrasonic treatment times on Fe grade and impurities phosphorous, alumina and silica for sample (G3).

Fig. (15) Effect of different ultrasonic treatment times on Fe grade and impurities phosphorous, alumina and silica for sample (G1).

Fig. (16) BSE images for sample G2. (A) and (B) BSE images of the original −500+250 μm size fraction of the feed sample show that phosphorus (P) and alumina (Ch) minerals attached and coated hematite (He) ooids grains. (C) and (D) BSE images of the same sample after ultrasonic treatment for 5 min, indicated that phosphorus and alumina particles have been detached or ″disintegrated″ after ultrasonic treatment.

Fig. (17) BSE images for sample G3. (A) and (B)BSE images of the original −500+250 μm size fraction of the feed sample show that gangues minerals Fluoroapatite (P) and chamosite (Ch) concentrated between ooids and coated hematite (He) grains. (C) and (D) SEM images of the same sample after ultrasonic treatment for 10 min, confirmed that preferential disintegration of gangues minerals (fluoroapatite and chamosite) from the surface of hematite grains.

Table (1) Chemical analyses (wt. %) for the three iron ore samples and selected size fractions from each sample

Sample code		TFe (%)	P_2O_5 (%)	CaO (%)	SiO_2 (%)	Al_2O_3 (%)	MgO (%)	F (%)
G1	Bulk sample	48,33	5,64	7,59	15,03	3,37	1,23	0,37
	+125 -250 µm	48,57	3,48	5,36	17,70	3,70	1,25	0,21
	+250 -500 µm	47,97	3,17	4,83	20,07	3,40	1,14	0,22
	+500 – 1000 µm	51,11	3,09	4,70	17,25	3,10	1,03	0,19
G2	Bulk sample	46,08	2,25	2,67	29,54	3,27	0,27	0,32
	+125 -250 µm	46,96	1,89	2,44	30,32	2,58	0,36	0,28
	+250 -500 µm	45,35	1,45	1,75	33,26	2,41	0,45	0,29
	+500 – 1000 µm	44,23	1,33	1,59	34,61	2,24	0,26	0,3
G3	Bulk sample	58,27	3,24	5,44	7,48	4,47	1,26	0,19
	+125 -250 µm	59,61	2,50	4,67	8,16	3,99	0,92	0,07
	+250 -500 µm	58,50	2,79	4,97	8,66	4,12	0,99	0,09
	+500 – 1000 µm	62,30	2,28	4,10	6,84	3,40	0,74	0,05

(G1) High phosphorus sample, (G2) Low phosphorus sample, (G3) Intermediate phosphorus sample.

Table (2) Mineralogical composition (wt. %) for the three iron ore samples and selected size fractions from each sample.

Sample code		Hematite (%)	Goethite (%)	Chamosite (%)	Fluoroapatite (%)	Quartz (%)
G1	Bulk sample	60,52	5,46	8,42	13,28	12,32
	+125 -250 µm	59,21	6,78	9,25	9,38	15,38
	+250 -500 µm	58,79	6,32	8,50	8,45	17,94
	+500 – 1000 µm	62,84	5,88	7,75	8,22	15,31
G2	Bulk sample	60,67	--	8,17	4,67	26,49
	+125 -250 µm	60,83	--	7,45	4,27	27,45
	+250 -500 µm	59,17	--	6,02	3,06	31,75
	+500 – 1000 µm	58,41	--	5,60	2,78	33,21
G3	Bulk sample	74,63	--	11,17	9,52	4,68
	+125 -250 µm	76,20	--	9,97	8,17	5,66
	+250 -500 µm	74,93	--	10,30	8,69	6,08
	+500 – 1000 µm	79,62	--	8,50	7,17	4,71

(G1) High phosphorus sample, (G2) Low phosphorus sample, (G3) Intermediate phosphorus sample.

Table (3) Heating properties of minerals with microwave radiation.

Mineral	Formula	Microwave Heating

Hematite	Fe_2O_3	Heat readily, but no mineral phase change (active)
Quartz	SiO_2	Does not heat (inactive)
Fluroapatite	$Ca_5(PO_4,CO_3)_3F$	Very little or no heat generated
Chamosite	$(Fe^{++},Mg,Fe^{+++})_5Al(Si_3Al)O10(OH,O)_8$	Very little or no heat generated

Table (4) Effect of microwave pretreatment on the percentages of fine material removed by ultrasonic treatment (15% pulp density, 10 min ultrasound time).

Sample	Grain size (μm)	Disintegration materials (%)	
		With microwave pretreatment (900 W, 60 s)	Without microwave pretreatment
G1	+125 -250 μm	10.84	9.74
	+250 -500 μm	8.33	7.42
	+500 – 1000 μm	2.59	2.39
G2	+125 -250 μm	15.48	12.44
	+250 -500 μm	14.88	10.78
	+500 – 1000 μm	4.52	2.52
G3	+125 -250 μm	14.62	12.22
	+250 -500 μm	11.92	8.34
	+500 – 1000 μm	3.92	2.49

Table (5) Products grades and recoveries of Fe, P_2O_5, Al_2O_3 and SiO_2 after ultrasonic treatment followed by de-sliming.

Sample code	**Exp. conditions**		**Fe %**	**P_2O_5 %**	**SiO_2 %**	**Al_2O_3 %**	**Fe Recovery (%)**	**P_2O_5 Removal (%)**	**Al_2O_3 Removal (%)**
G1	Grain size (+250 -500 μm), sonication time (10 min), pulp density (15%).	Product	48,66	2,58	17,48	2,42	93,09	18,61 % (F) 54,25 % (G1)	28,82% (F) 28,18% (G1)
		Feed sample	47,97	3,17	20,07	3,40			
		Sample HPS	48,33	5,64	15,03	3,37			
G2	Grain size (+250 - 500 μm), sonication time (5 min), pulp density (15%).	Product	48,32	0,71	29,62	1,18	94,29	59,42 % (F) 68,44 % (G2)	51,03% (F) 63,91% (G2)
		Feed sample	45,35	1,45	33,26	2,41			
		Sample LPS	46,08	2,25	29,54	3,27			
G3	Grain size (+250 - 500 μm),	Product	60,85	1,88	7,22	2,86	91,61	32,61 % (F) 41,97 % (G3)	30,58% (F) 36,02% (G3)

sonication time (10 min), pulp density (15%).	Feed sample	58,50	2,79	8,66	4,12
	Sample IPS	58,27	3,24	7,48	4,47

(F) Feed sample with grain size (+250 -500 µm), (G1) Bulk high phosphorus sample, (G2) Bulk low phosphorus sample, (G3) Bulk intermediate phosphorus sample.

Table (6) Products mineralogical composition (wt. %) for the three iron ore samples after ultrasonic treatment followed by de-sliming.

Sample code	Exp. conditions		Hematite %	Goethite %	Chamosite %	Fluorapatite %	Quartz %
G1	Grain size (+250 - 500 µm), sonication time (10 min), pulp density (15%).	Product	65,60	5,85	6,25	6,88	15,42
		Feed sample	58,79	6,32	8,50	8,45	17,94
		Sample HPS	60,52	5,46	8,42	13,28	12,32
G2	Grain size (+250 - 500 µm), sonication time (10 min), pulp density (15%).	Product	71,39		2,95	< 1	24,66
		Feed sample	59,17	--	6,02	3,06	31,75
		Sample LPS	60,67	--	8,17	4,67	26,49
G3	Grain size (+250 - 500 µm), sonication time (10 min), pulp density (15%).	Product	82,04	--	7,21	5,91	4,84
		Feed sample	74,93	--	10,30	8,69	6,08
		Sample IPS	74,63	--	11,17	9,52	4,68

(F) Feed sample with grain size (+250 -500 µm), (G1) Bulk high phosphorus sample, (G2) Bulk low phosphorus sample, (G3) Bulk intermediate phosphorus sample.

Table (7) Effect of pulp density on the percentages of disintegration materials after ultrasonic treatment for 10 mins.

Sample	Grain size (µm)	Pulp density (%)		
		15%	30%	45%
		Disintegration materials (%)		
G1	+125 -250 µm	10.84	8.69	7.35
	+250 -500 µm	8.33	6.74	5.44
	+500 – 1000 µm	2.59	1.88	1.45
G2	+125 -250 µm	15.48	12.88	10.22
	+250 -500 µm	14.88	11.22	9.65
	+500 – 1000 µm	4.52	3.88	3.32
G3	+125 -250 µm	14.62	11.92	10.44
	+250 -500 µm	11.92	10.32	8.66
	+500 – 1000 µm	3.29	2.42	1.75

Figure 1

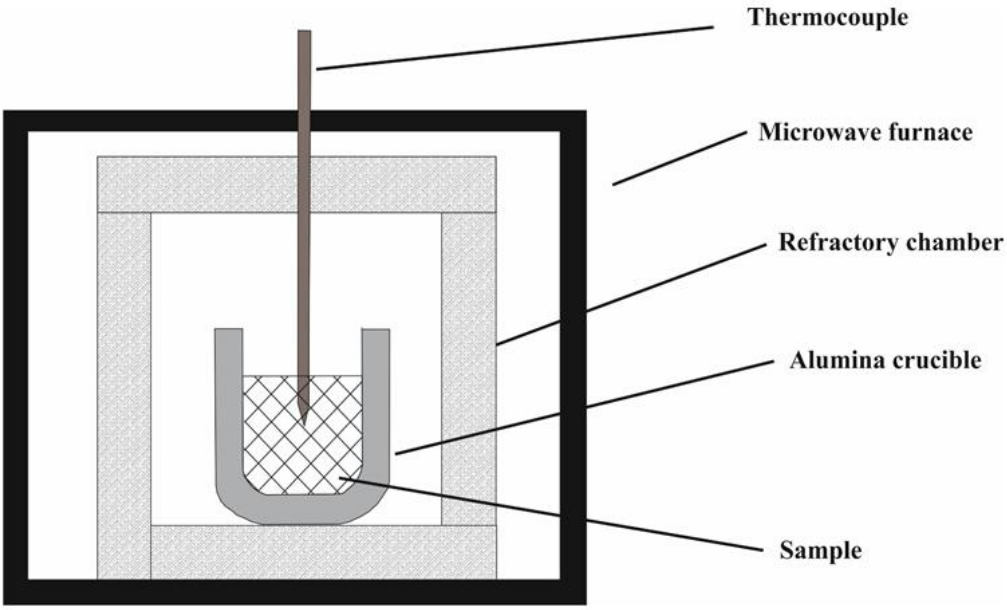

Figure 2

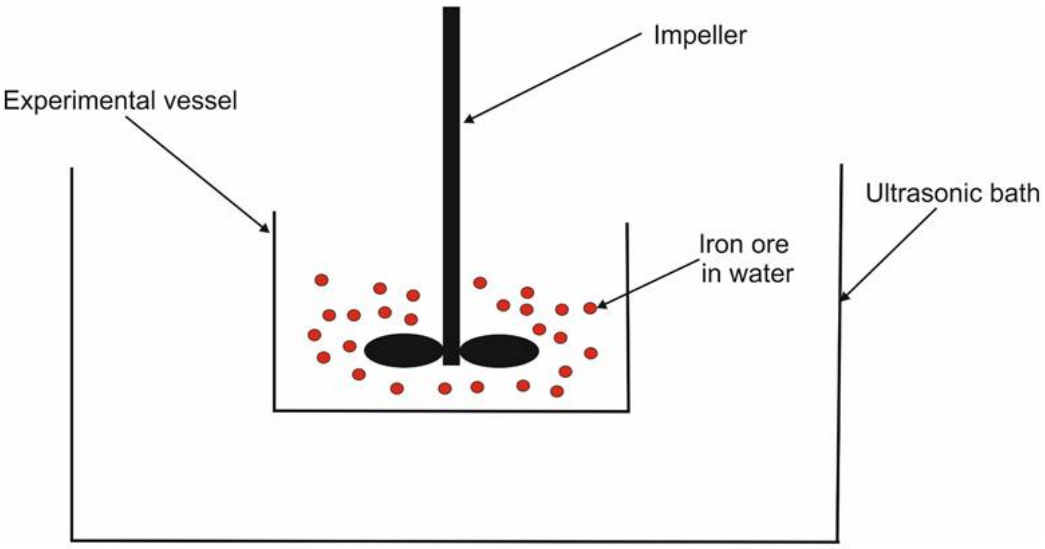

Figure 3

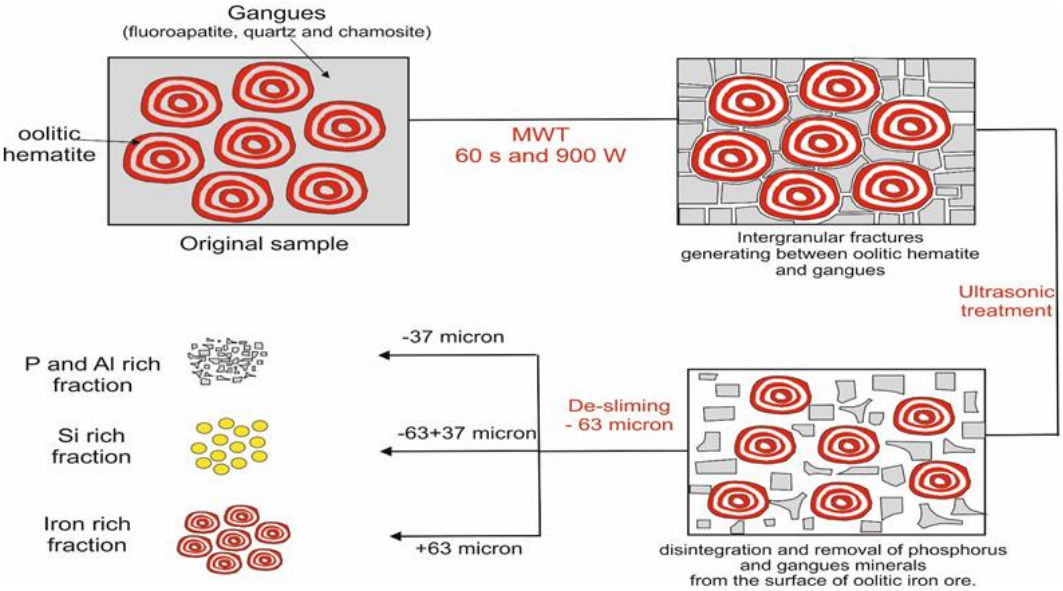

Figure 4

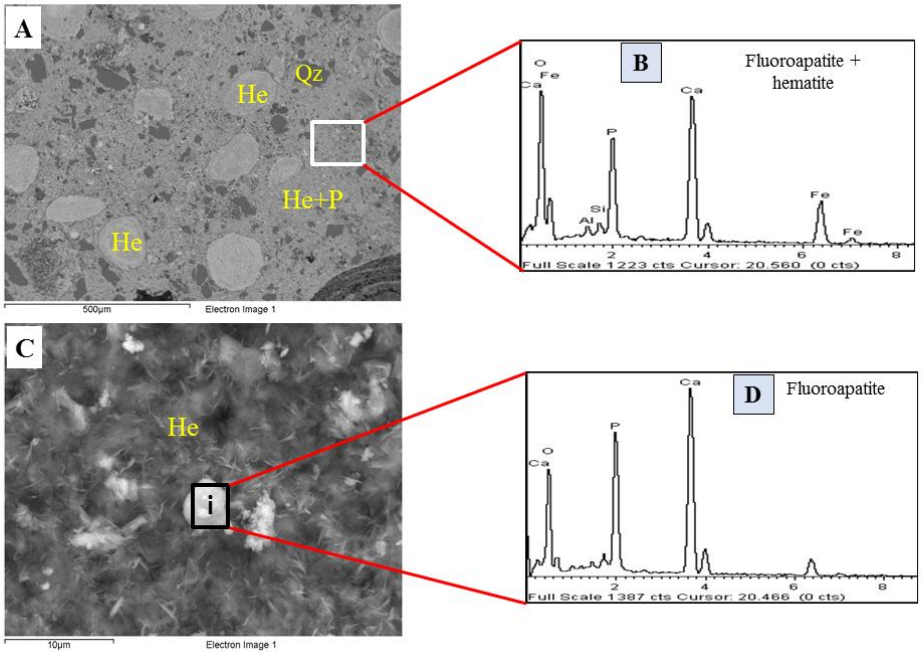

Figure 5

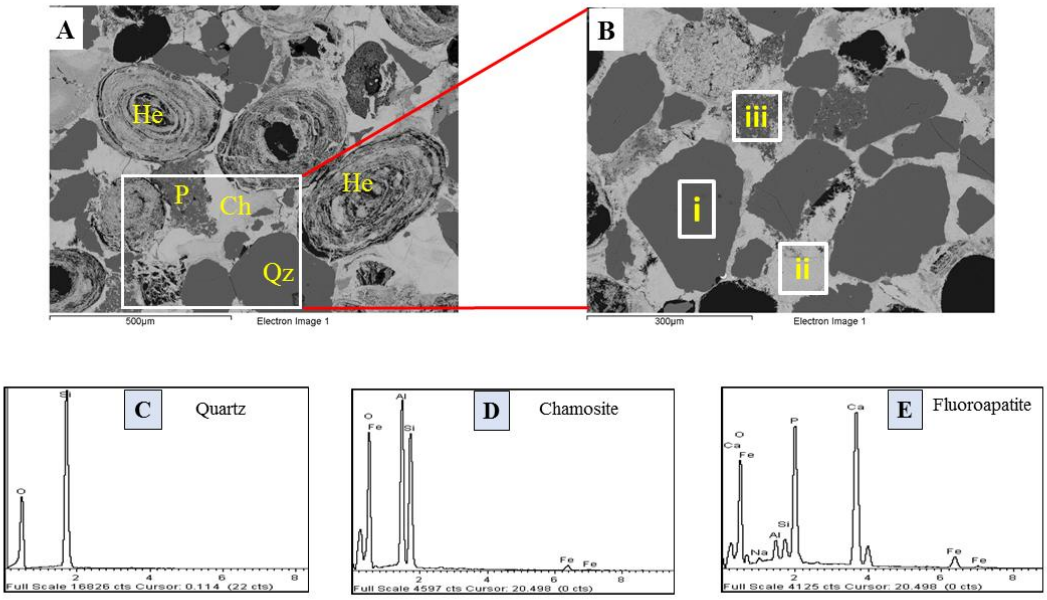

Figure 6

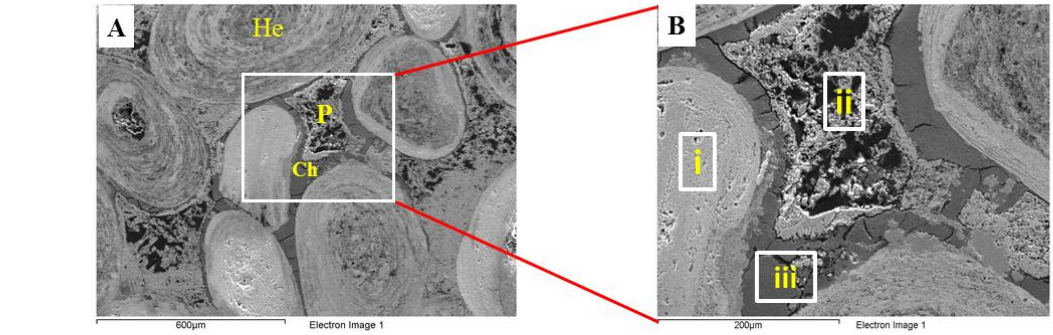

Figure 7

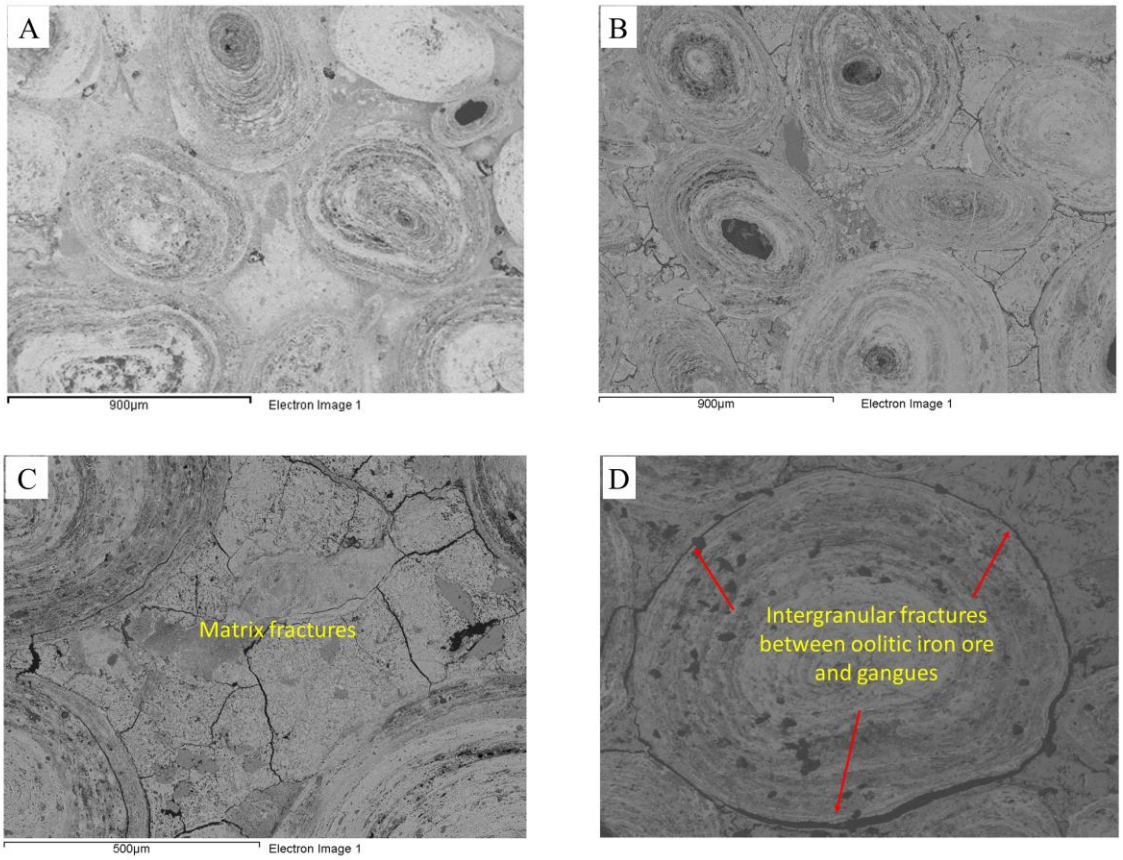

Figure 8

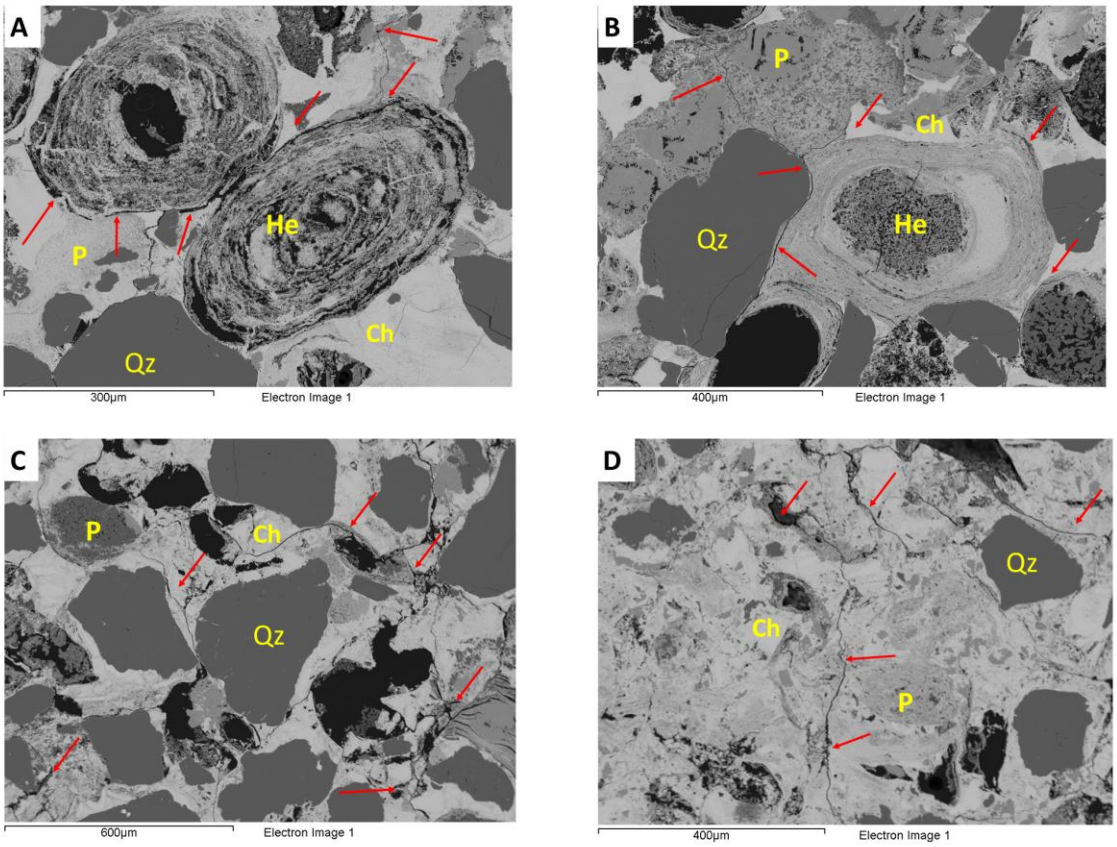

Figure 9

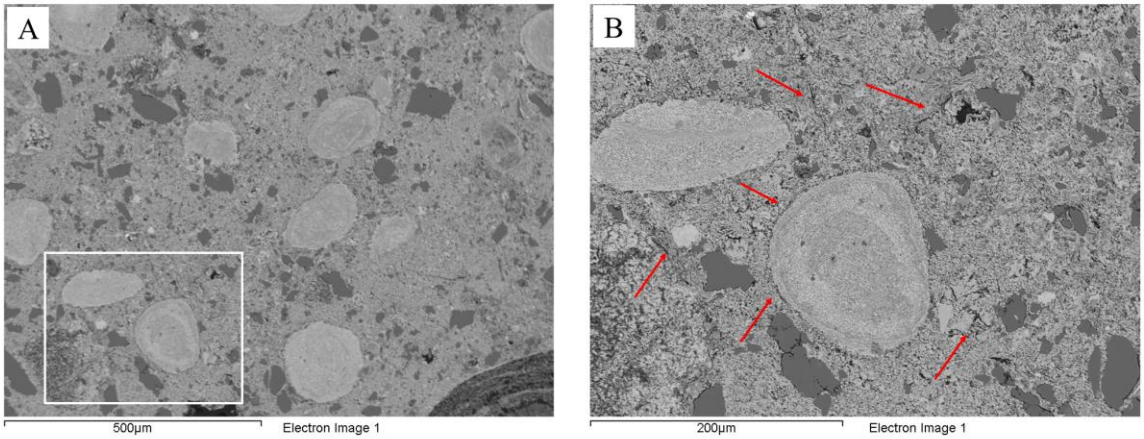

Figure 10

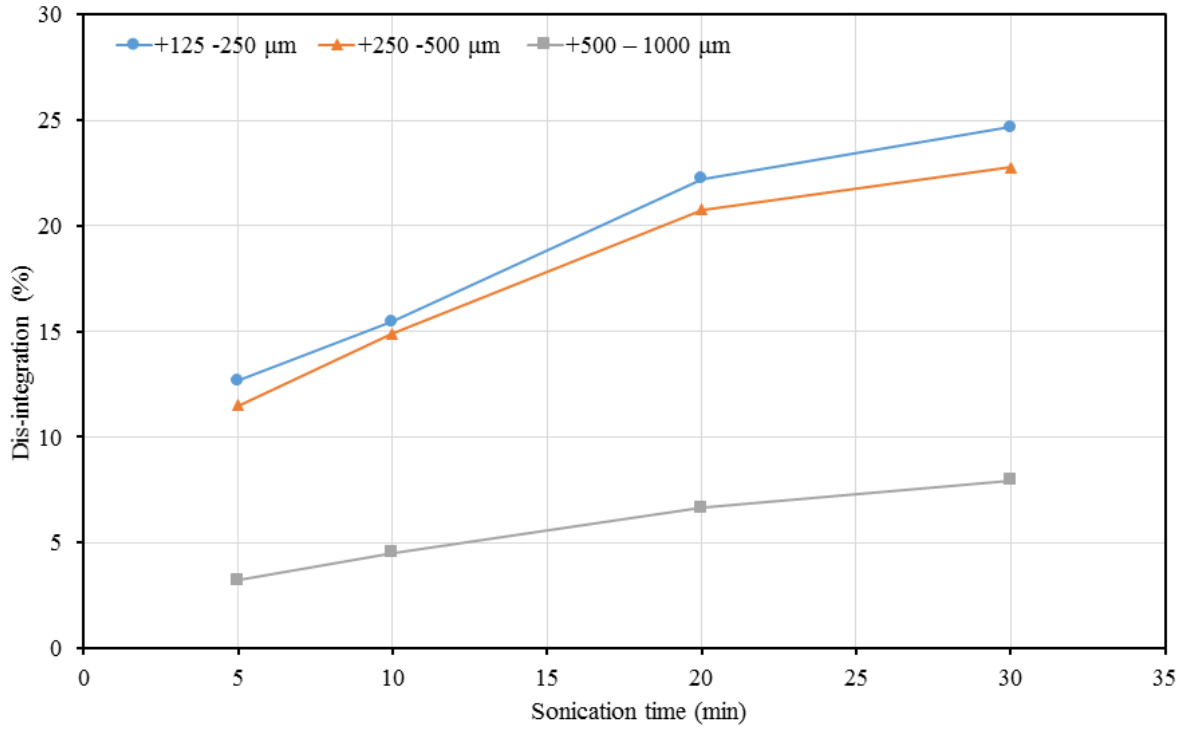

Figure 11

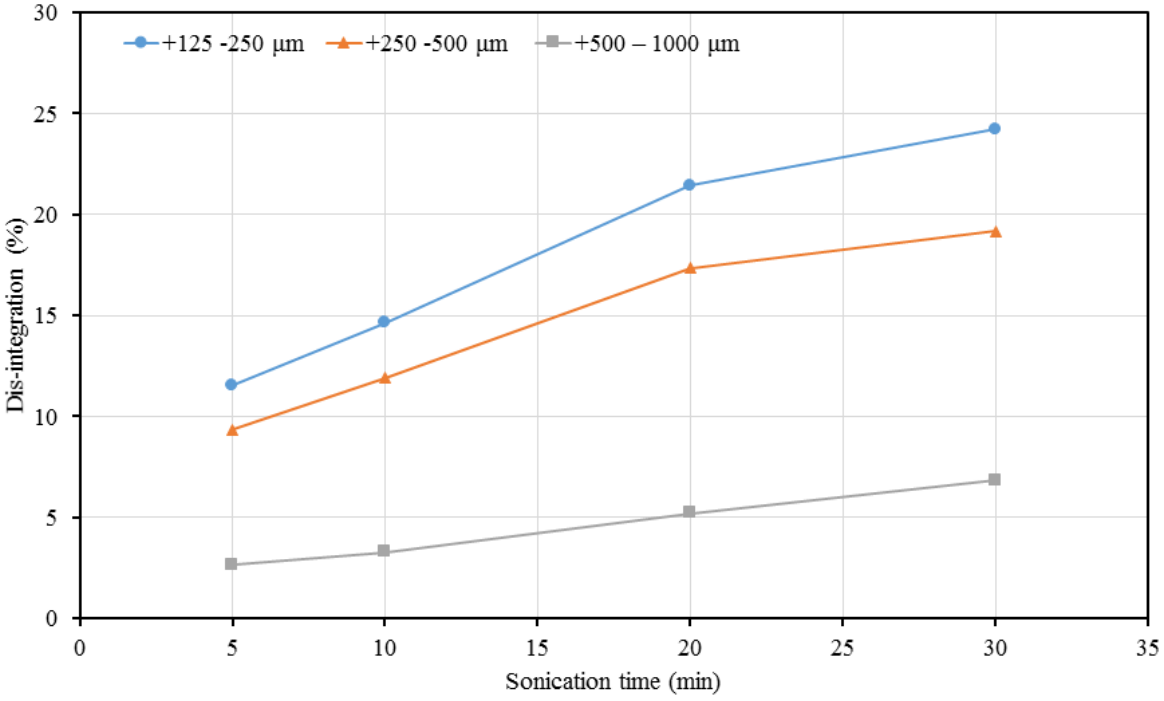

Figure 12

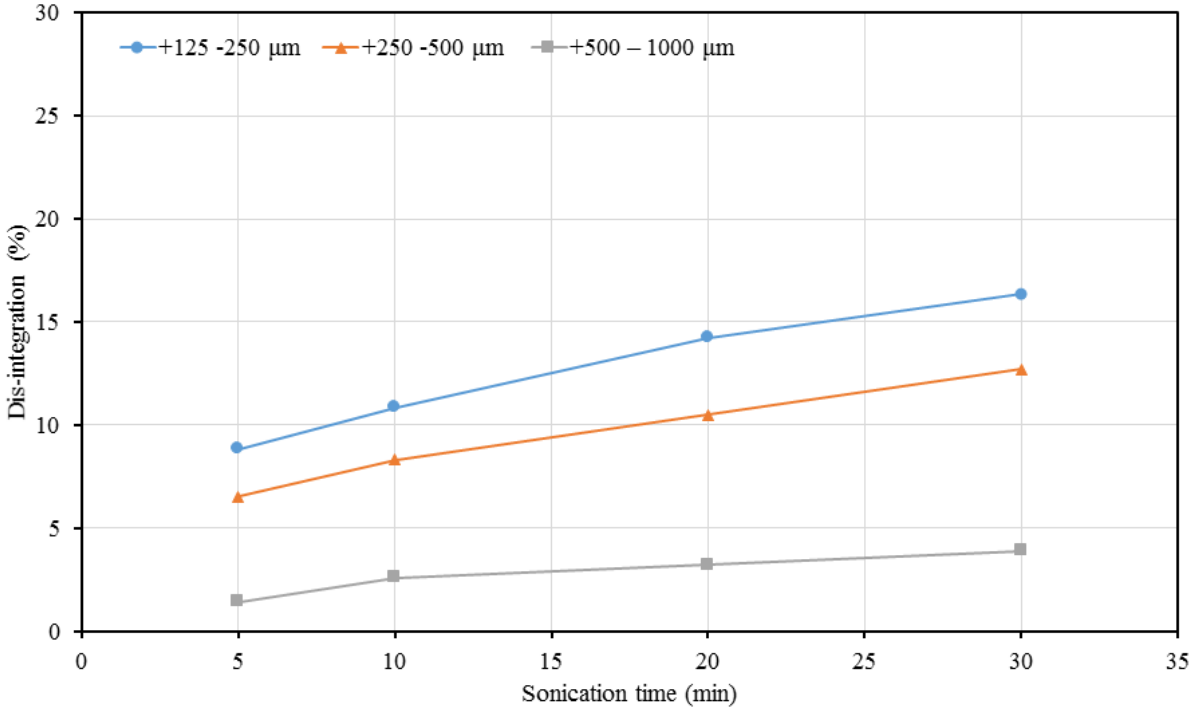

Figure 13

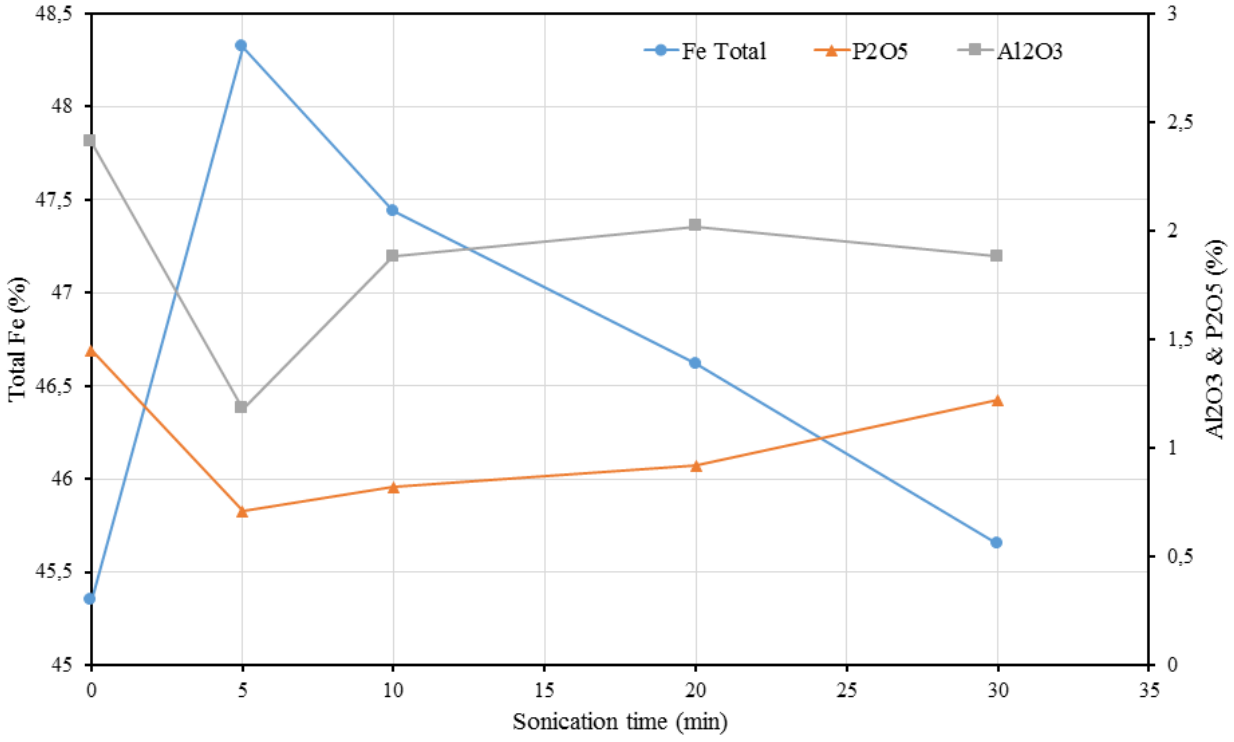

Figure 14

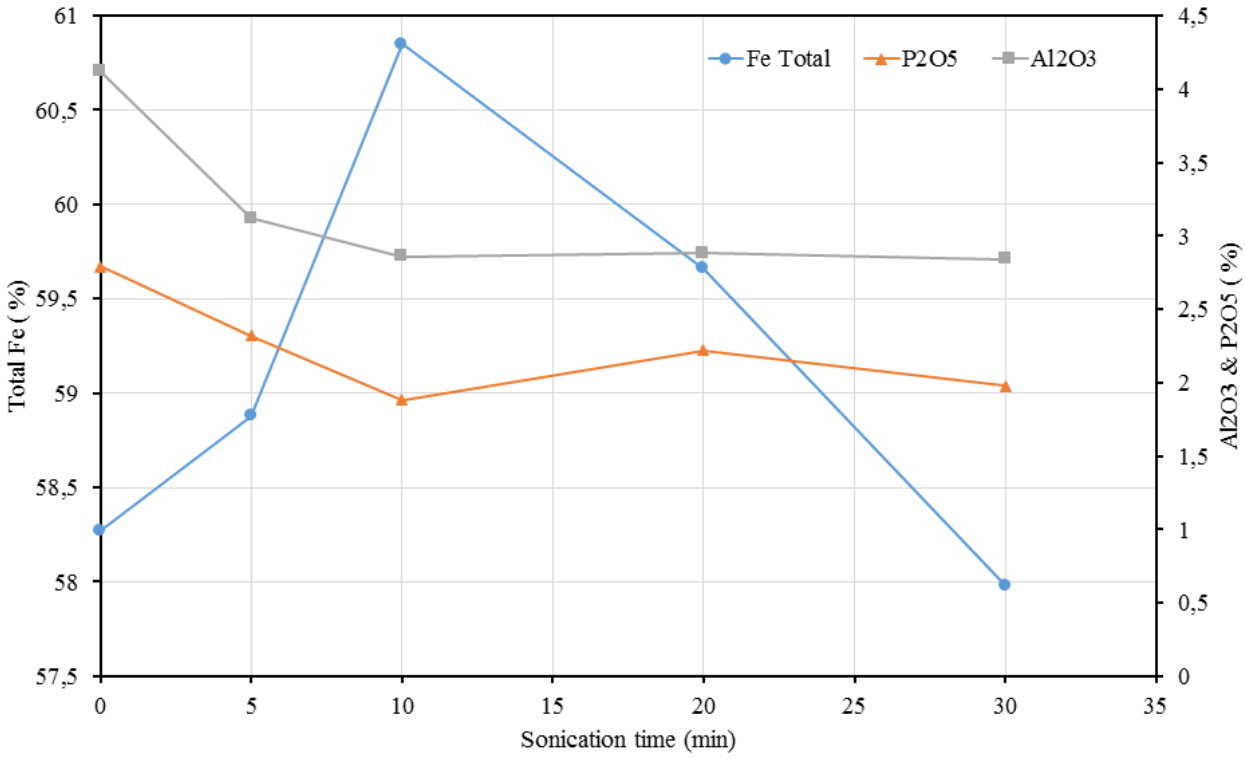

Figure 15

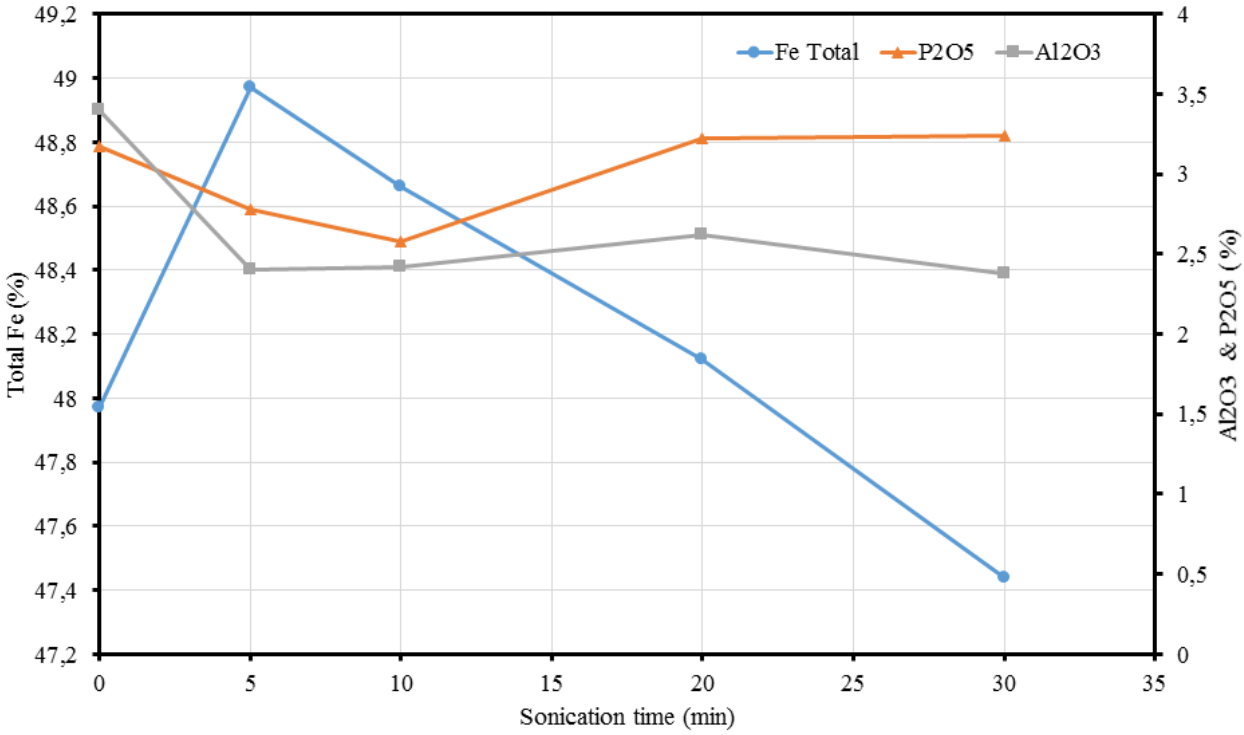

Figure 16

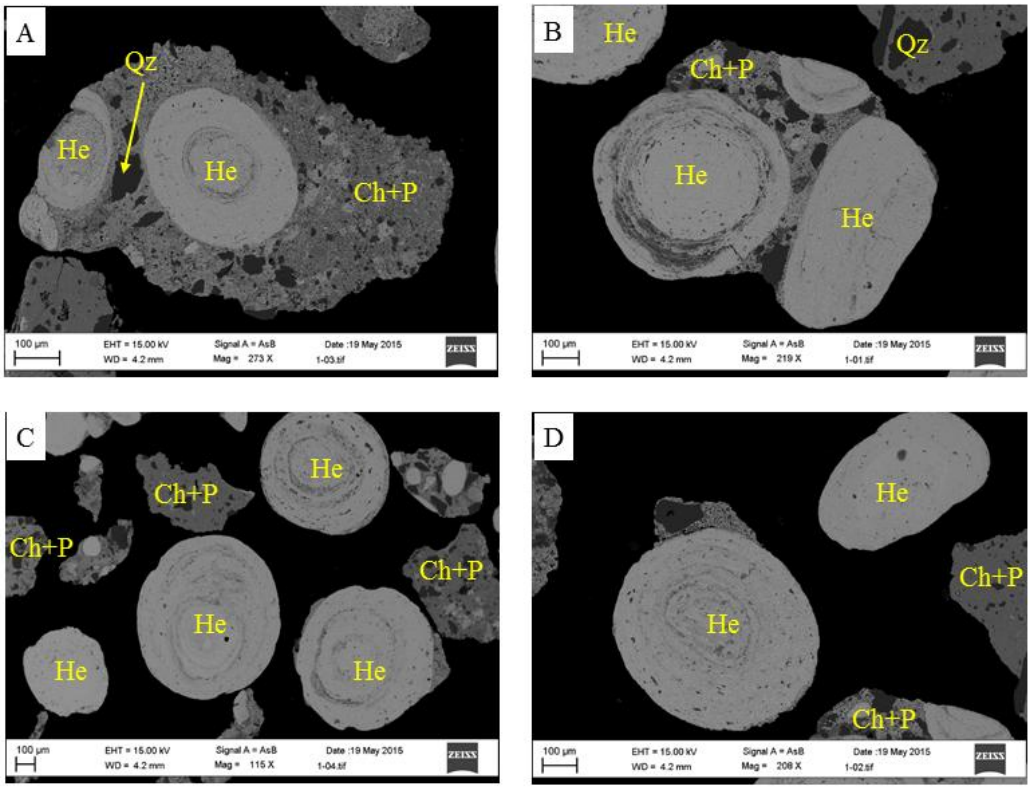

Figure 17

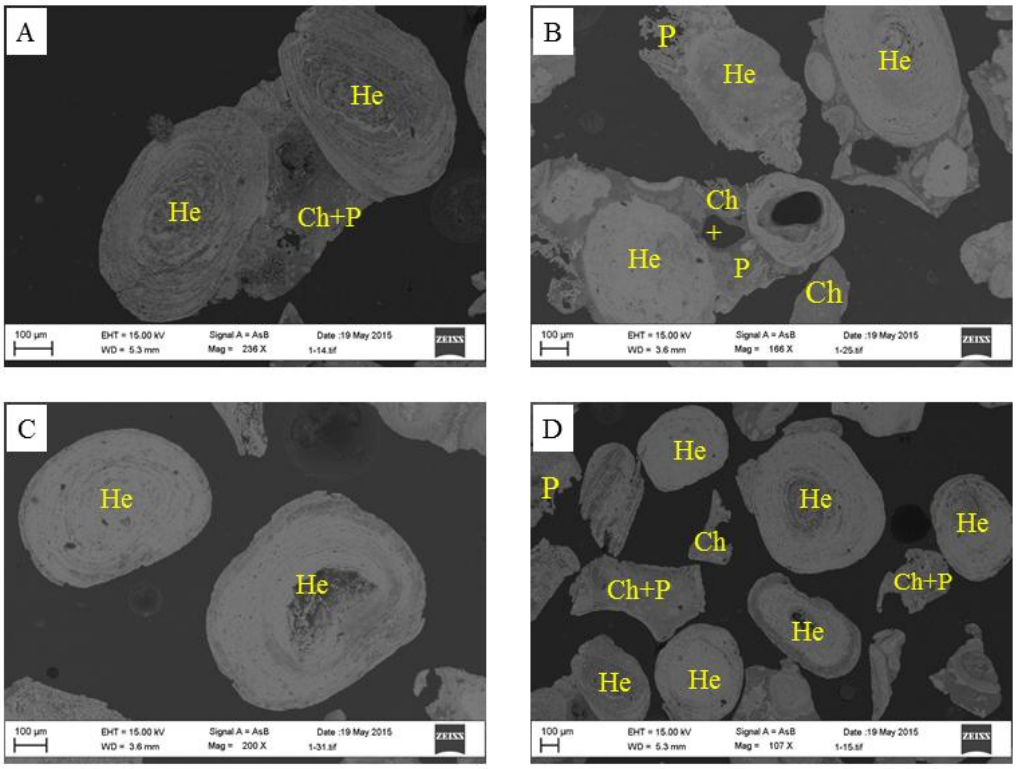

Graphical Abstract

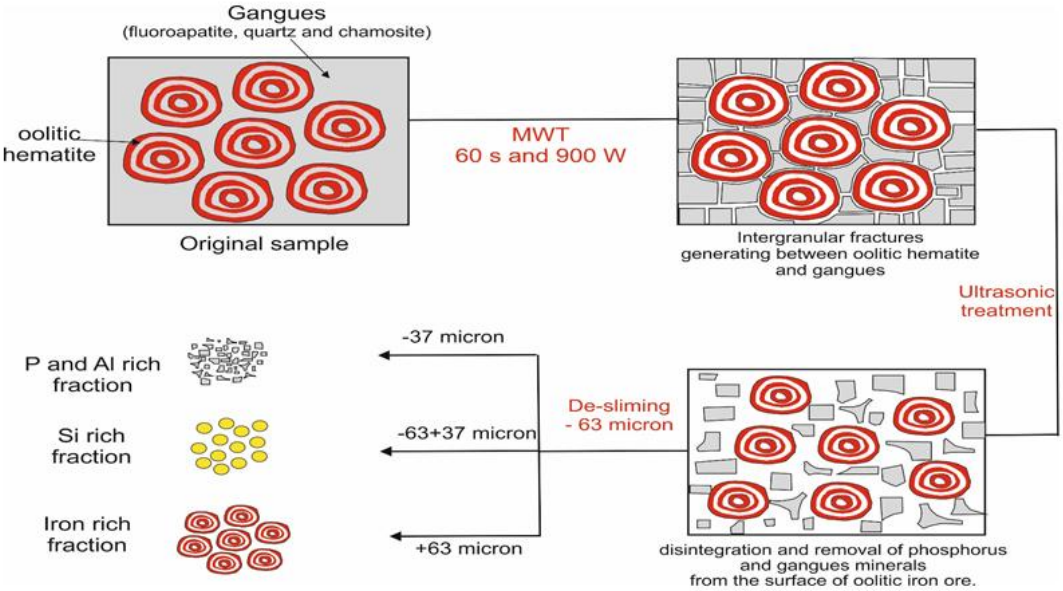

Highlights

- The effect of combined microwave pretreatment and ultrasonic treatment on the removal of phosphorus from iron ore was studied.
- The results indicated that microwave pretreatment increases the efficiency of ultrasonic disintegration of particles by about 20% compared to untreated sample.
- Sample texture and degree of phosphorus liberation affect the efficiency of phosphorus removal.
- The improvement in Fe grade and the decrease in impurities after ultrasonic treatment is attributed to the disintegration and removal of fine gangue components.